UCRL-ID-131942

Coupling Measurement and Lightning Threat Assessment Report for Pantex Cell 12-44-1

Mike Ong
Robert Anderson

September 1998

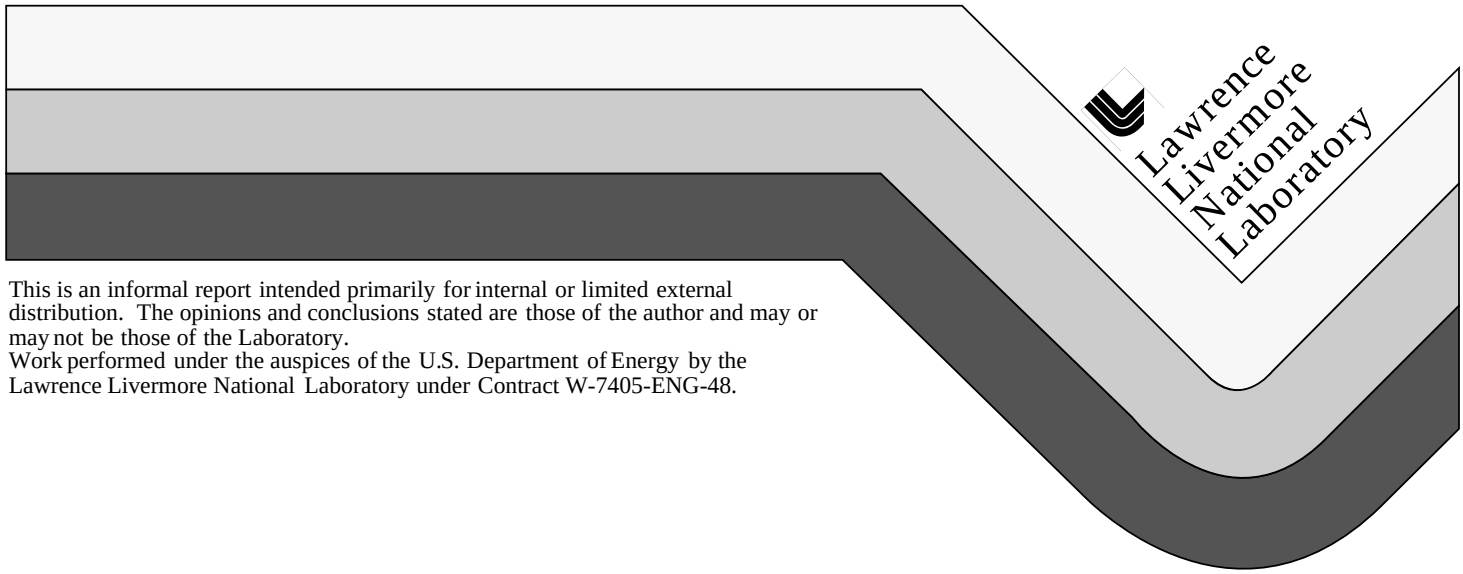

Coupling Measurement and Lightning Threat Assessment Report for Pantex Cell 12-44-1

Mike Ong
Robert Anderson
September 1998
(925) 422-0206

Lawrence Livermore National Laboratory

Table of Contents

Summary

This report is the first of a series that will quantify the lightning threat to the Pantex Plant where high-risk operations occur. More information can be found in the report written by the Lightning Protection Team [1] and Sandia National Laboratory documents.

Low-power RF coupling measurements were completed on Cell 12-44-1 in May 1998. These measurements quantify the voltage and current levels that could leak into the cell from possible lightning strike points. Cell 1 is representative of the most "leaky" class of cells at Pantex because the floor was not intentionally electrically connected to the walls. From the measurement data, linear models were developed. These transfer functions allow us to calculate the effect in the cell from the much higher power lightning threat.

Two types of coupling paths were characterized: (1) external ventilation stack to cell interior and (2) cell ceiling to other cell elements. For the maximum lightning threat [2], an estimate of the maximum cell-to-floor voltage is **150 kV**. The extrapolated voltage levels at normal working heights are lower. The potential between the air duct and the electro-static ground is estimated to be **4 kV**.

A secondary goal was to compare results with Sandia as a quality control check. While the estimated maximum ceiling-to-floor voltages are similar, the comparison was limited by high-frequency resonances on the drive wire.

Introduction

The main objective of the measurement was to provide data to estimate the voltage threat in the cell. The threat consists of lightning energy that leaks through the "Faraday cage". If sufficiently high, this energy could generate an arc that delivers enough voltage and current to initiate a detonator. Because of the importance of the threat assessment, we also wanted to compare our results with those from Sandia.

Estimation of the lightning threat can be broken into three phases: low-power measurements, data processing to produce transfer functions, and extrapolation. They must all be considered in planning the measurement. For this cell, Sandia and Livermore agreed to check the data processing phase of the threat calculation.

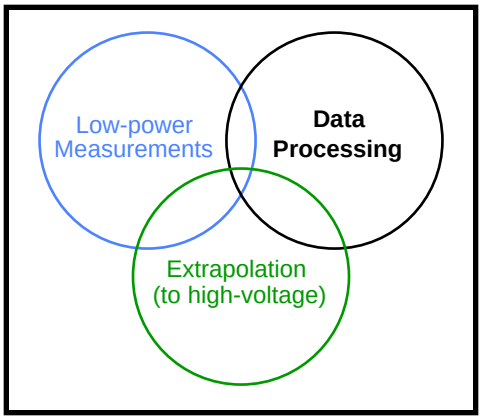

Figure 1. The three phases of threat estimates.

Measurement Strategy

Four factors determine the design of our measurement matrix. (1) We must determine the likely strike points (2) that have the best coupling paths to metallic penetrations in the cells. These serve as the injection points. (3) In the cell we must select penetrations that could be near a detonator. This serves as one-half of the receiver input. (4) The other half is the return path or "ground". The electrical fields in the cell are also recorded to calculate ceiling-to-floor voltages.

Strike Points and Coupling Paths

There are numerous possible lightning strike points that could force energy into Cell 1. After inspection of the cell and the surrounding environment, we identified two attachment points associated coupling paths that would likely convey the highest level of voltage and current into the cell. (1) The ventilation stacks on the roof supply air into the cell through an equipment room. This path may not be electrically contiguous because of isolating flexible couplings in the ductwork. However, the separation is about one and one half inches and an

electrical arc could easily be created that would conduct current into the cell. We can simulate these arcs with small wire jumpers. (2) Lightning could strike the top of the roof and force energy through the earth into the ceiling of the cell. Unlike "Faraday cage", the earth does not conduct well and its conductance would likely become nonlinear when struck by lightning. At least in the upper portion of the path, the earth as a dielectric would break down from the high voltages driven by the lightning. The resulting arcs in the earth form a lower conductance path. This type of coupling path with a non-linear response segment cannot be measured with low-power equipment. Contrastingly, the coupling path in the cell will likely have a linear response. The exception is the possible discontinuity at the floor and wall joint. The top of the cell was not accessible from the outside. Therefore, we will measure the coupling from the ceiling inside the cell to penetration points near possible detonator locations and the cell fields. The non-linear issues will be discussed further in the extrapolation of the measurement results.

Cell Penetrations and Return Paths

There are three metallic penetrations in the cell that could pose a threat to detonators. (See Figure 2.) Point A -- The air duct comes into the cell just above the entrance. Point B -- Pressurized air is supplied by a metal pipe that goes around the cell. Given its length and serpentine path, the pipe might transport energy around the cell. Point C -- The crane is attached at the top of the cell and the lifting chain could carry voltages down into the workspace. The crane was tested in the normal "parked" position.

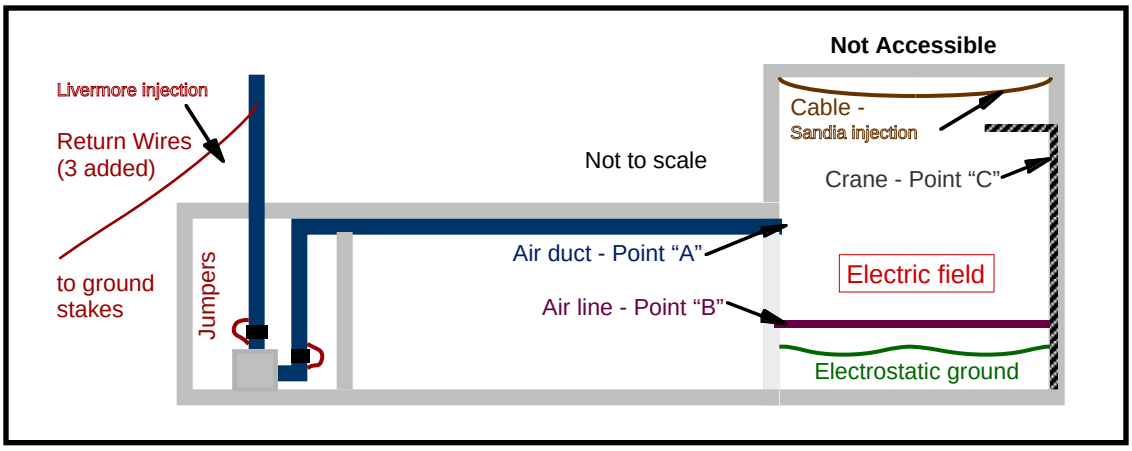

Figure 2. Cell 12-44-1 injection and measurement points.

There are many possible return paths or "grounds". The obvious one is the steel mesh in the concrete. However, the mesh is not exposed at any point and therefore is difficult to include in the measurements. Any of the penetrations could be a return path. However, we selected the electrostatic ground as the return path. It is attached to the cell rebar and the grounding system outside. The electrostatic ground is a good reference point.

The electric field was measured in a number of locations on, or close to the floor. The currents in the cell rebar and metallic penetrations drive the electrical field. Hence, they are related.

Measurement Setup

The measurement equipment configuration is shown in Figure 3. Currents are injected with an inductively coupled loop. The source steps through the frequency range that covers the spectrum of the worst case lightning threat: 10 kHz to 2.56 MHz in 10 kHz steps. The injected current is measured with a second inductive loop sensor. In the cell, the receiver consists of two

spectrum analyzers. They are computer controlled to reduce the measurement time. The frequency setting of the source and spectrum analyzers must be synchronized to obtain a very high signal-to-noise ratio. This is done with the clocks in the two computers. Noise floor measurements using the different sensors are made by turning off the RF source.

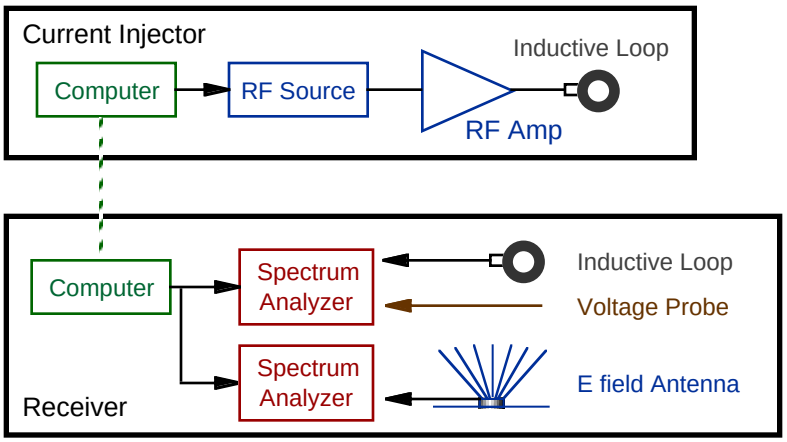

Figure 3. Test equipment configuration for coupling measurements.

The equipment list can be found in Appendix A. Photographs of the equipment are shown in Figure 4. The current sensors and electric field antenna were calibrated at LLNL. The sensitivities were very close to the published specifications. The antenna factor (13 V/m / V) was constant over the frequency range of interest. The inductively coupled current loops (with nominal sensitivity of 1V / A) were less sensitive at the lowest frequency and the data corrected in the data reduction.

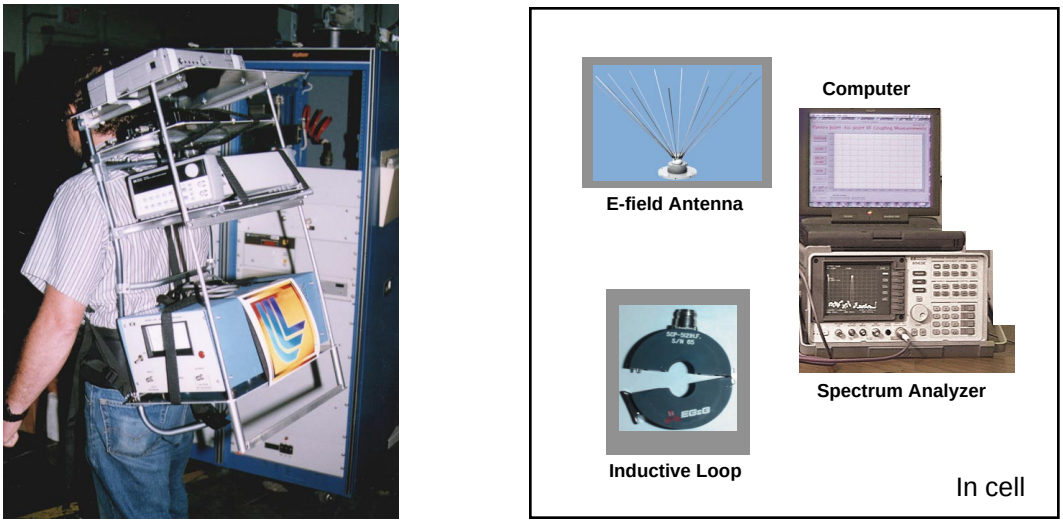

Figure 4. Photographs of low-power coupling measurement equipment.

LLNL repeated the cell field measurement performed by Sandia for a consistency check. We drove their wire attached to the ceiling inside the cell with our inductive loop.

Measurements Results and Data Reduction

The objective of data reduction is to produce the transfer functions that will be required for extrapolation. The raw measurements are shown in Appendix B. The first group shows the coupling from the ventilation stack into the cell. The second group of coupling measurements was generated with the internal Sandia injection wire. They have several resonance peaks that are not indicative of the cell response. While we were injecting on the external stack, the internal wire was temporarily connected and the same type of resonances appeared in the data. The spectrums of the injected currents at the ventilation and cell ceiling are shown in Appendix C.

The process for constructing the transfer functions is shown in the upper portion of Figure 5. All the measurements are made in the frequency domain. This technique provides exceptional signal-to-noise ratios given the safety requirement that limits the power of the RF source. The other important component is the spectrum analyzer operating with an extremely narrow-band receiving window. The sensors are calibrated with network analyzers. The lower portion describes the steps for extrapolating from low-power measurements to the high-power lightning threat. The calculations are done with a software package (SODA) developed at LLNL. It has been used for many years by the weapons testing programs. The transfer functions with the highest coupling are given in Appendix D.

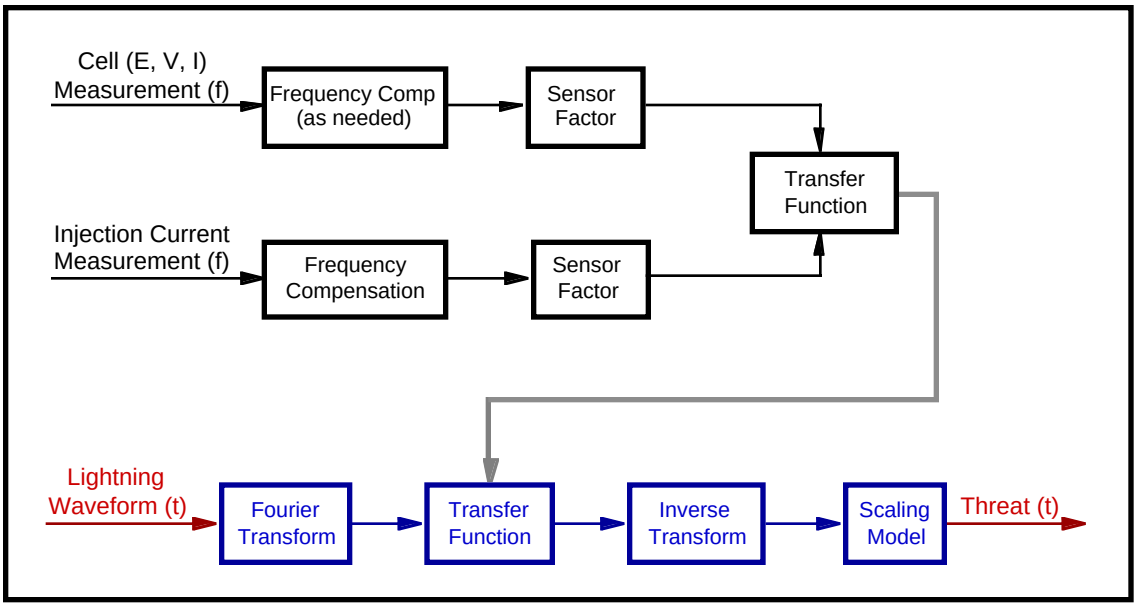

Figure 5. The data processing and extrapolation phases of lightning threat assessment.

In general, the coupling through the ventilation stack into the cell was less than from ceiling to the floor or penetrations. This was expected. The vertical electric fields were higher than the horizontal ones. Again, this was expected since we were injecting from the top. For the penetrations, Point A (the air duct) produced the highest coupling. The discontinuity of the entrance and height of the duct effect the amount of coupling. However, Point C (the crane) is lower than expected. This is a mystery.

Extrapolation Model and Threat Estimates

The extrapolation process is shown in the lower half of Figure 5. The first assumption is that the cell response is linear, e.g., doubling the injected current increases the cell voltage by two. This is true for a well-constructed “Faraday cage”. A well-constructed cage has no major electrical discontinuities. In Cell 12-44-1 our concern was the floor and wall connection. It is difficult to determine from the different waveforms the condition of the floor-wall joint.

However, the high extrapolated floor-to-ceiling voltage indicates that this cell has less shielding than other cells at Pantex.

Our analysis concentrates on the locations with the highest coupling. For the electrical field, readings were highest at the center of the cell. For the penetrations, the air duct (Point A) produced some of the highest coupling levels. As can be expected, the internal drive point produced the higher coupling levels. Our analysis did not include detailed computer modeling because the cell will likely need to be "fixed".

The cell voltage as predicted by the electrical field measurements was highest while injecting on the Sandia wire. It was connected to the ceiling inside the cell. The external injection point produced lower fields. This is consistent with our understanding of coupling theory. The current injected onto the ventilation stake must travel a longer path to the cell and thus provide more opportunity for the current to drain off in other directions.

The threat lightning waveform is defined by a double exponential. (See Figure 6.) The peak current is 200 kA. The rate of rise is 400 kA/µs. The full-width-half-maximum (FWHM) is 100 µs. This threat is considered extreme and should occur in less than 1% of the strikes at Pantex.

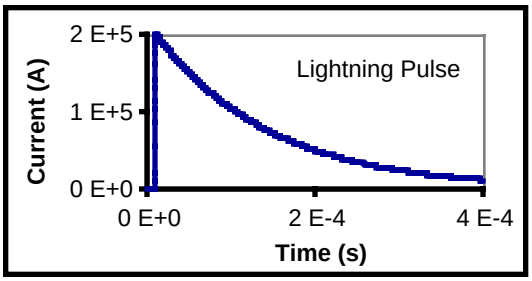

Figure 6. Lightning profile for simulation.

The transfer function and the estimated floor-to-ceiling voltage are shown in Figure 7. The transfer function contains information out to 2.5 MHz. However, we have removed the high frequency resonances because they are artifacts created by the drive wire and not indicative of the cell response. The estimated inductance is 40 nH. It impedance is shown as the solid line. The measured data points are shown in red.

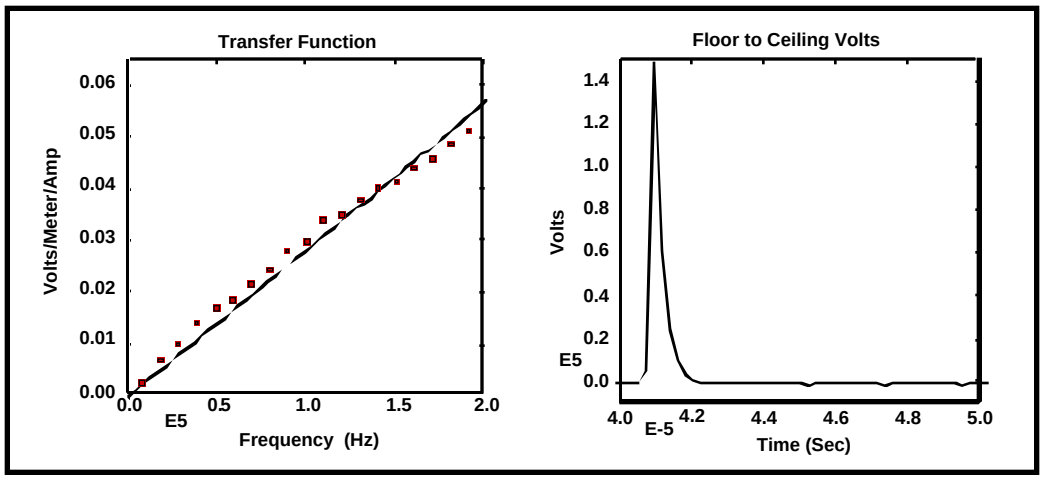

Figure 7. Transfer function for electrical field in cell and extrapolated voltage threat.

The peak cell voltage is about 150 kV. We assumed that the electric field is uniform in the vertical dimension. Therefore, we multiplied the field level by the height (6 meters) to get the cell voltage. Given that the discontinuity is likely at the floor-to-wall joint, this is a conservative approach to scaling. Note that the pulse width is much narrower than the lightning pulse. This is characteristic of an inductive structure.

The effect of resonances is shown in Figure 8. They tend to ride on top of the cell voltage and cause an over estimation.

In theory, if lightning were to strike the top of the cell, the induced voltage will distribute evenly over the cell. (See Figure 9.) However, joints, metallic penetrations and holes distort the distribution. Nonetheless, we would expect that voltage levels with respect to the floor on penetrations at the normal working heights, to be less than ceiling voltage. This is the case with the air duct, also known as Point A.

The coupled voltage at the air duct was measured with the spectrum analyzer that has an input impedance of 50Ω. The transfer impedance is shown in Figure 10. We believe that the data in only the lower frequency band is valid.

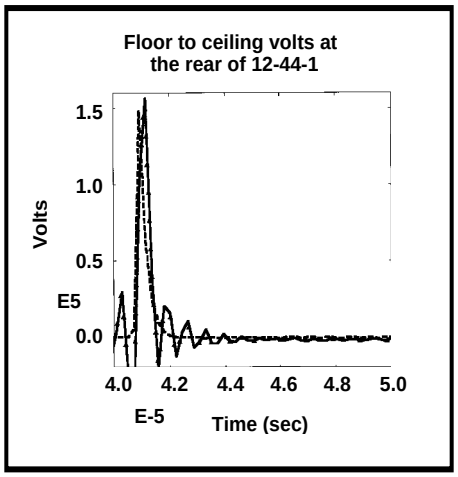

Figure 8. Extrapolated cell voltage with and without resonances.

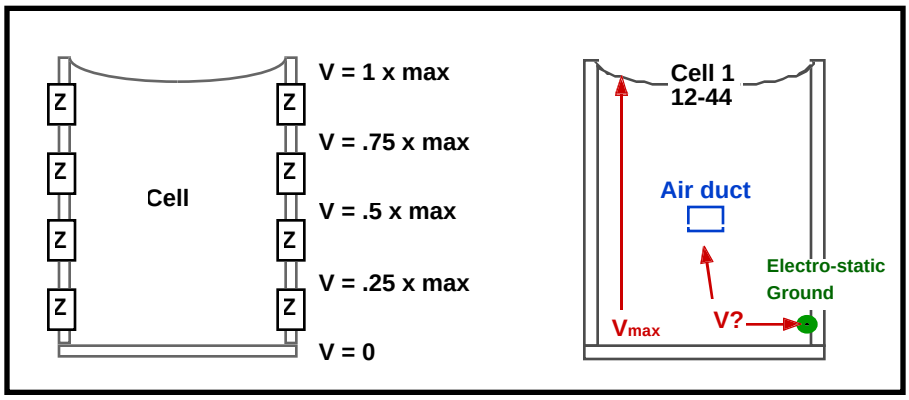

Figure 9. Ideally voltages uniformly distribute themselves along the wall. Real cells, however, only somewhat follow this pattern.

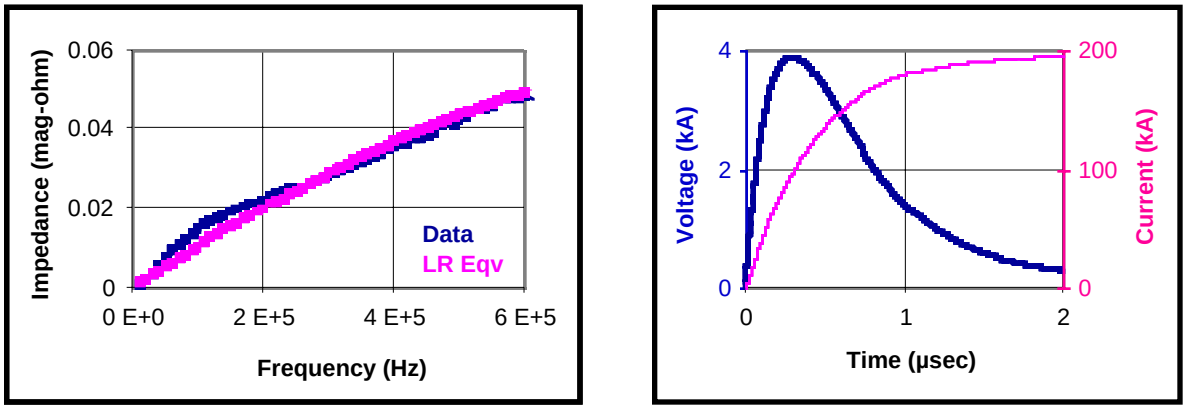

Figure 10. Transfer function for voltage at air duct and extrapolated threat.

The transfer impedance can be modeled with a simple circuit. It would consist of an inductor (16 nH) in parallel with a resistor (.08). A very small resistance (.9 mΩ) was added to the inductor to generate a conservative estimate of the transfer function at DC. The extrapolated voltage was computed with Micro-Cap, a circuit simulation program. It was low, 4 kV with respect to electrostatic ground. (See Figure 10.) The rising edge of lightning current profile is also shown. The electrostatic ground cable was 17 inches off the floor. The air duct was 7 feet from the floor. The cell height is about 16 feet. Given these dimensions, the expected voltage should have been higher. A possible explanation may be that the voltage drop is concentrated at another location. Nonetheless, the expected voltage levels at normal working heights are lower than the ceiling-to-floor voltage.

If an arc does form between a metallic penetration and a detonator, it will only initiate if there is sufficient current. This can be determined with another transfer function. We added a jumper with a small gage wire (#16) to connect the penetration to the ground point. The jumper simulates the arc path through air. A current probe measures the current in the jumper wire while the strike point is driven. The strike point is the ceiling of the cell. The resulting transfer function is shown in Figure 11. This short-circuit current has a profile similar to the lightning shape. It was computed with the signal processing package in MATLAB. The high-frequency ringing should be ignored and is an artifact of the drive wire. Therefore the peak current is approximately 600 A, and is enough to initiate some detonator.

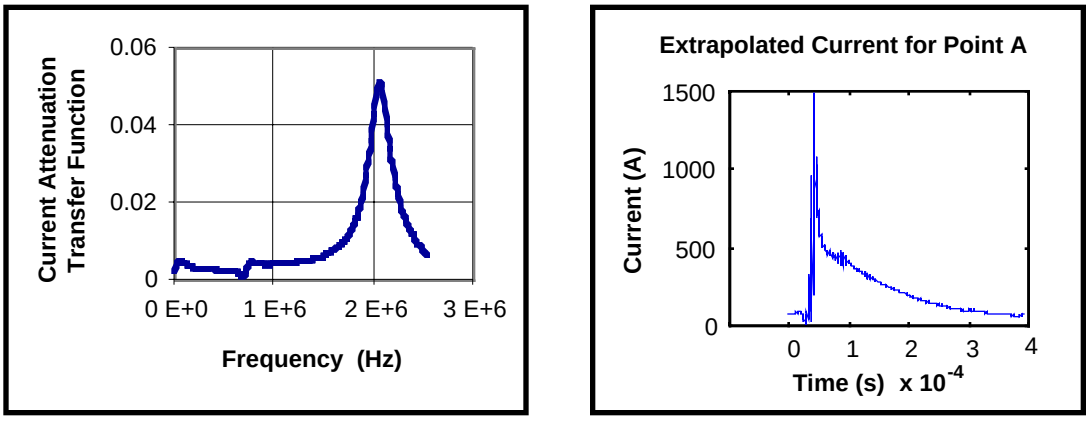

Figure 11. Transfer function for current at air duct and extrapolated current threat.

Conclusions and Recommendations

The penetrations in Cell 12-44-1 are unbonded and the floor-wall joint is possibly electrically disconnected. These conditions are consistent with estimated maximum cell voltage of 150 kV. However, this voltage level should only be considered an estimate because of the possible non-linear response of a disconnected floor-wall joint. This discontinuity could allow arcs to form inside the concrete leading to spalling.

We therefore recommend the following actions before performing high-risk operations

- Bond all penetrations
- Connect the floor and wall which may require digging into the concrete
- Retest the cell

The maximum voltage level induced by a lightning strike at penetrations at normal working heights was estimated to be about 4 kV. We expect this safety margin will still exist after improving the integrity of the cell.

Acknowledgment

We gratefully acknowledge the work of Trish Walsh and Alan Scruggs. Their insight, planning, coordination, and hard work were crucial to the success to the measurements. Jim Dunlap had the difficult job of running the injector while exposed to the elements. He also did much of the preparation including the calibrations. Aaron Jones wrote the software which allowed us to take a large number of measurements. We also wish to thank Lei Loni Rodrigues for her work in the preparation of the presentations and this report. We especially want to thank Dr. Marvin Morris for his insight in the extrapolation process.

References

[1] Lightning Protection Project Team, "Analysis of the Risk Presented by Lightning in the Pantex Nuclear Explosives Areas Lightning Protection Project Team", to be issued by Bob Young, DOE Amarillo Office.

[2] Fisher, R. J., M. A. Uman, "Recommended Baseline Direct-Strike Lightning Environment for Stockpile-to-Target Sequences", Sandia Report, May 1989, SAND89-0192.

Appendix A - Equipment List

Equipment Type	Model	Frequency	Notes
Spectrum Analyzers	Tektronix - 8563E Tektronix – 8561E*	9 kHz - 26.5 GHz 30 Hz – 6.5 GHz	*Second unit borrowed from HP
RF Source	HP - 33120	100 µHz - 15 MHz	
RF Amplifier	ENI - 240L	20 kHz - 10 MHz	40 watts
E-field Sensor	Tecom - 201191 A	20 Hz - 100 MHz	Band 1 (low)
Current Sensor	EG&G - SCP-1 LF	12 kHz - 70 MHz	3 dB
Computers	Toshiba - Notebooks		
Software	National LabView	NA	Written at LLNL

Appendix B - Raw Coupling Data for Cell 12-44-1 Taken on May 20-21, 1998

This appendix contains most of the raw data taken on Cell 12-44-1 on July 21, 1998. These are not transfer functions. Some of the patterns in the waveforms were created by the changes in injection current. The first three plots are the results of injecting current on the external ventilation stack. The last three consist of measurements made with the internal drive wire. For a given type of drive, relative comparisons of different test points are valid. Note the excellent signal-to-noise ratio except at the higher frequencies.

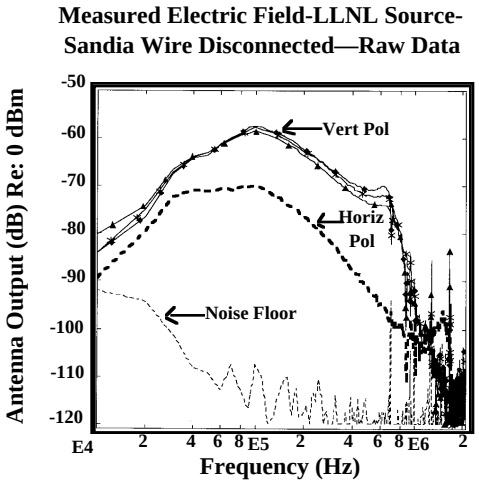

Figure B1. Electric field in cell driven by injection onto external air stack with Sandia cell wire disconnected.

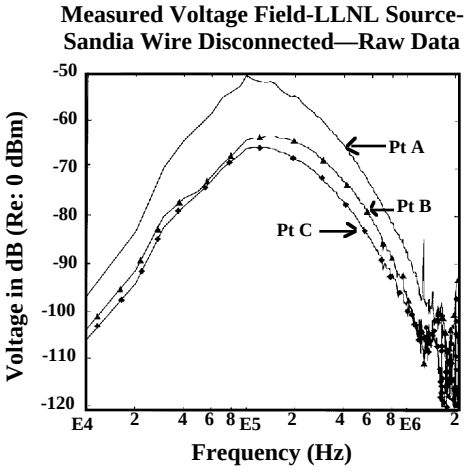

Figure B2. Voltages on cell penetrations driven by injection onto external air stack with Sandia cell wire disconnected.

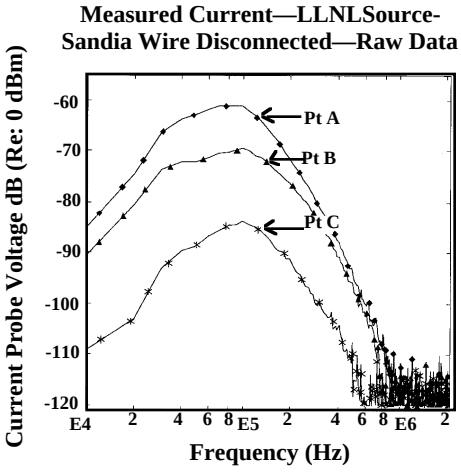

Figure B3. Currents on cell penetrations driven by injection onto external air stack with Sandia cell wire disconnected.

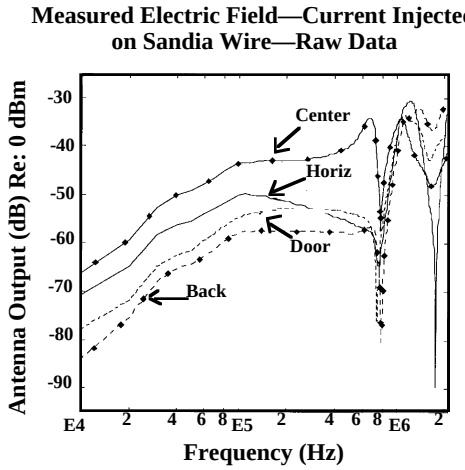

Figure B4. Electric field in cell driven by injection onto ceiling of cell with Sandia wire.

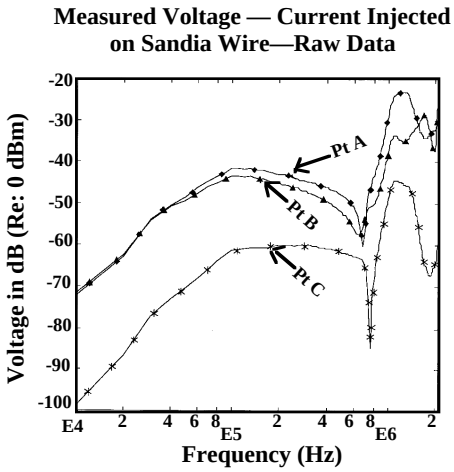

Figure B5. Voltages on cell penetrations driven by injection onto ceiling of cell with Sandia wire.

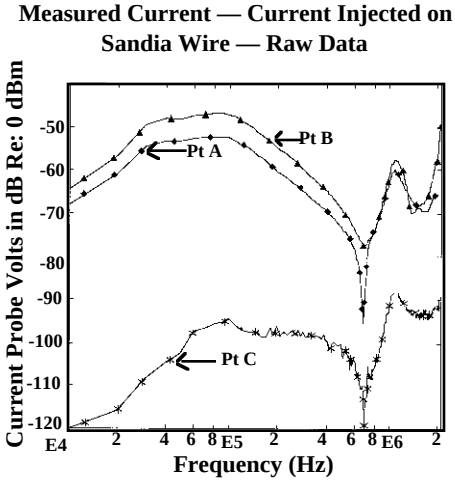

Figure B6. Currents on cell penetrations driven by injection onto ceiling of cell with Sandia wire.

Appendix C – Currents Injection Spectrums

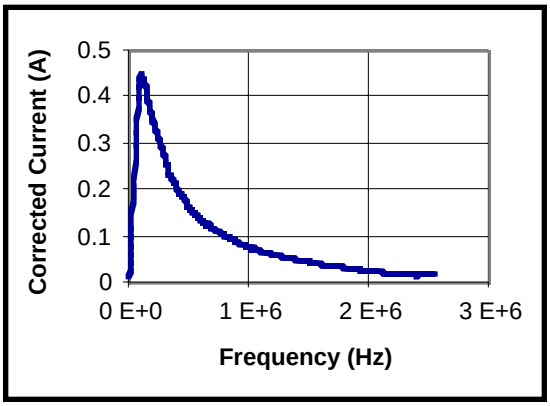

Figure C1. Spectrum of current injected onto external ventilation stack.

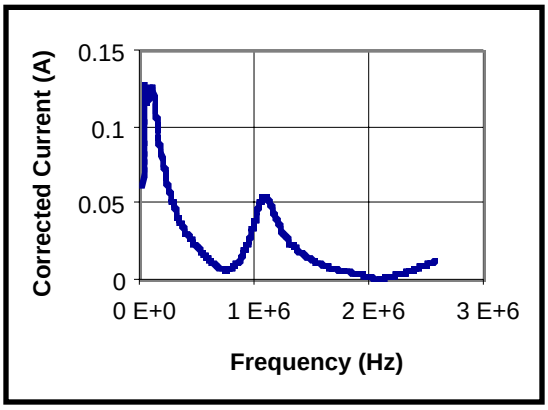

Figure C2. Spectrum of current injected onto Sandia wire in cell.

Appendix D – Transfer Functions for Cell 12-44-1

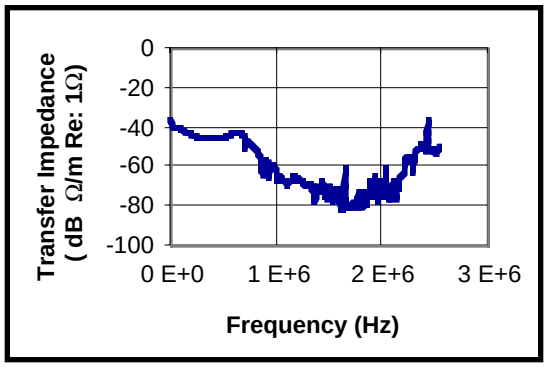

Figure D1. Transfer impedance at back of cell with external ventilation drive.

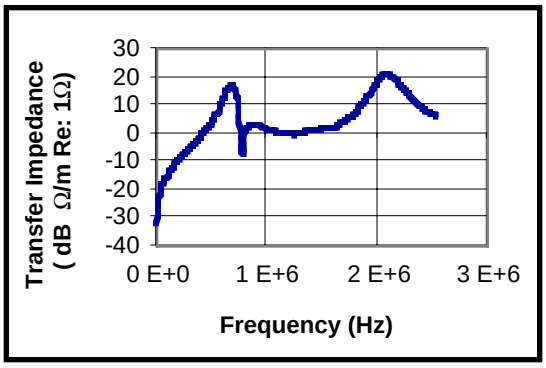

Figure D2. Transfer impedance in center of cell using internal Sandia drive wire.

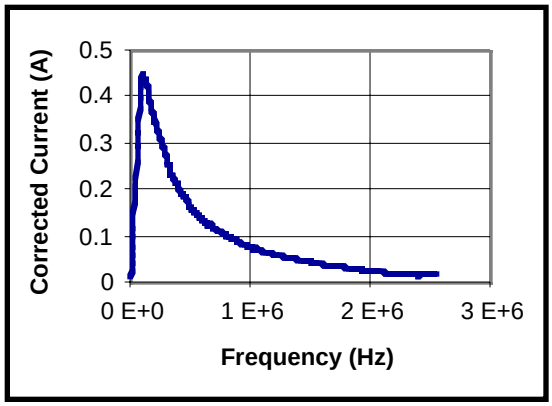

Figure D3. Voltage transfer function for air duct (Point A) using internal Sandia drive wire.

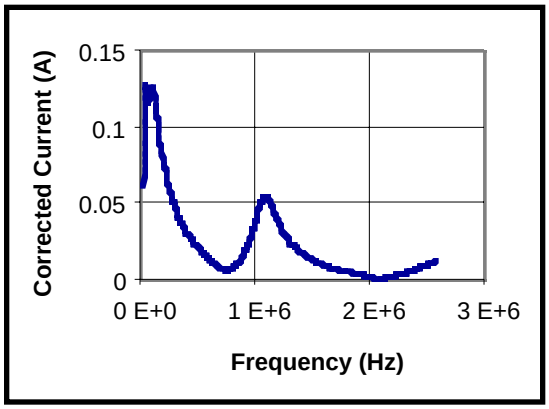

Figure D4. Current transfer function for air duct (Point A) using internal Sandia drive wire.

Appendix E – Comparison of SNLA and LLNL Measurement Techniques

While there are some differences in the measurement and data processing techniques between SNLA and LLNL, both should give equivalent results. Figure E1 shows the difference in injection approach, voltage versus current. However, since the injected current is measured. They are equivalent. Livermore measures more parameters (four) and records more data points (256) assisted by the computer. The data processing is shown in Figure E2.

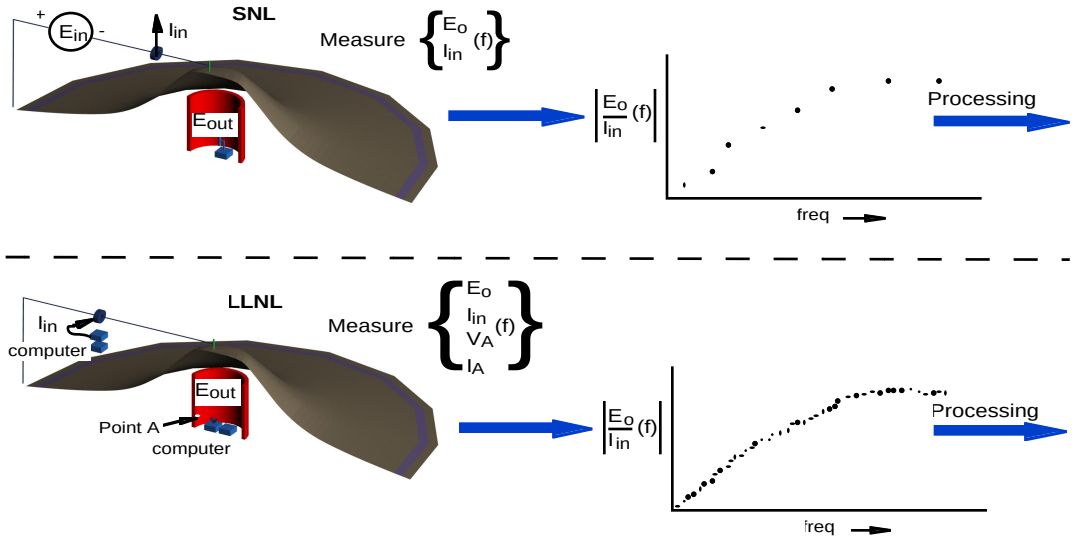

Figure E1. SNLA and LLNL measurement techniques are different but should produce similar results.

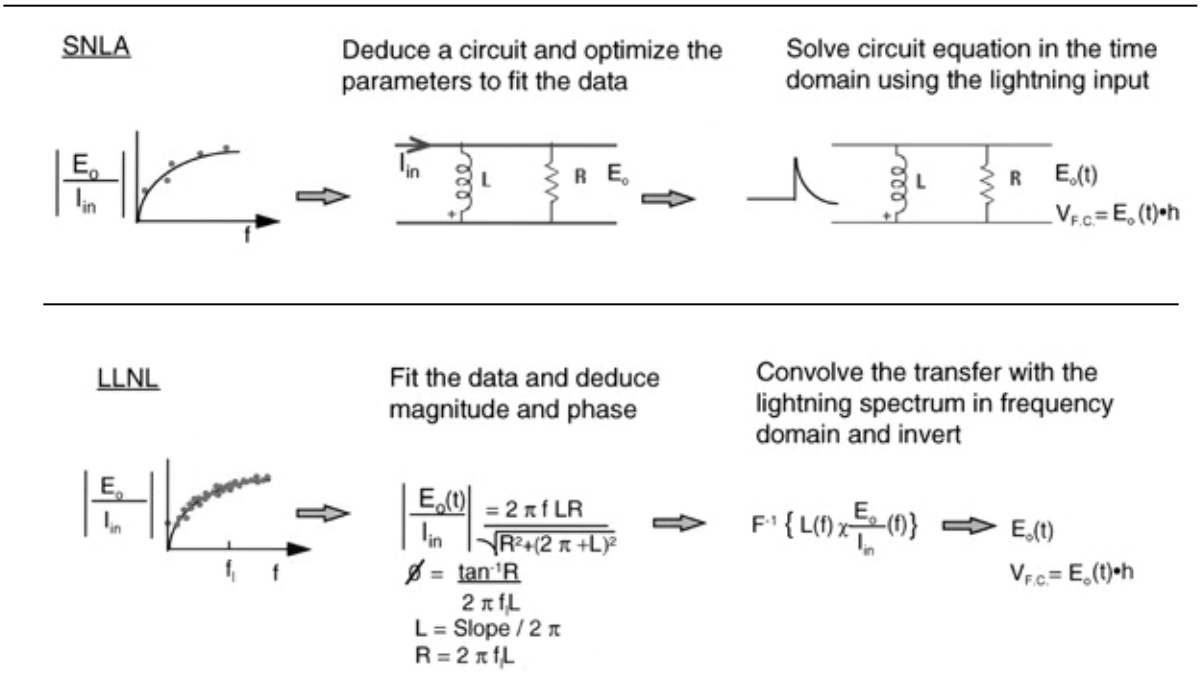

Figure E2. SNLA's circuit modeling and LLNL's signal processing techniques for data processing.